

NATIONAL ADVISORY COMMITTEE FOR AERONAUTICS

TECHNICAL NOTE 2531

SIMPLIFIED METHOD FOR CALCULATION OF COMPRESSIBLE
LAMINAR BOUNDARY LAYER WITH ARBITRARY
FREE-STREAM PRESSURE GRADIENT

By George M. Low

Lewis Flight Propulsion Laboratory
Cleveland, Ohio

Reproduced From
Best Available Copy



Washington

October 1951

20000731
180

DISTRIBUTION STATEMENT A
Approved for Public Release
Distribution Unlimited

DTIC QUALITY INSPECTED 4

AQM00-103241

1

NATIONAL ADVISORY COMMITTEE FOR AERONAUTICS

TECHNICAL NOTE 2531

SIMPLIFIED METHOD FOR CALCULATION OF COMPRESSIBLE
LAMINAR BOUNDARY LAYER WITH ARBITRARY
FREE-STREAM PRESSURE GRADIENT

By George M. Low

SUMMARY

The Kármán-Pohlhausen integral method, as applied to compressible laminar boundary layers, was simplified by an analysis similar to the incompressible Holstein-Bohlen method. Although this simplification is helpful for many calculations, it is of greatest value when conditions at the edge of the boundary layer are known from experimental measurements. The analysis was conducted under the assumptions of a Prandtl number of 1, zero heat transfer, and a linear viscosity-temperature relation; velocity profiles are approximated by a fourth-degree polynomial.

Results are presented so that velocity and temperature profiles, momentum and displacement thicknesses, and wall shear stress can be calculated for flows over two-dimensional bodies with arbitrary free-stream velocity distributions. The results are also applicable to flows over three-dimensional bodies with axial symmetry through the use of Mangler's transformation.

INTRODUCTION

Present-day theory of compressible laminar boundary layers permits the aerodynamicist to make satisfactory boundary-layer calculations for flows with zero pressure gradients. Exact solutions of the boundary-layer equations for flows with streamwise pressure gradients, however, exist only for several specific pressure distributions (reference 1). Solutions of the laminar-boundary-layer equations for flows with arbitrary pressure gradients are of ever increasing importance because it has been suggested that at sufficiently high altitudes and speeds laminar boundary layers can exist at very high Reynolds numbers (reference 2), and because the pressure gradients encountered over most wings and bodies are not approximated by any of the aforementioned exact solutions.

The lack of exact solutions for flows with arbitrary streamwise pressure gradients necessitates the use of approximate solutions. The Kármán-Pohlhausen method has long been found to yield satisfactory solutions for incompressible flows, provided that the separation point is not approached. Howarth (reference 1) has recently applied this method to compressible flows.

The solution of the incompressible or compressible boundary-layer equations by the Kármán-Pohlhausen method is complex because it involves the numerical solution of a cumbersome differential equation, and because it involves second derivatives of the free-stream velocity, which cannot be determined with any accuracy if the free-stream velocity is known only from experimental measurements. For incompressible fluids, these difficulties have been overcome by the Holstein-Bohlen simplification (reference 3), which eliminates the second derivatives of the free-stream velocity and simplifies the differential equation.

In the present report of an analysis made at the NACA Lewis laboratory, the Holstein-Bohlen simplification is applied to the Kármán-Pohlhausen method for compressible fluids. The momentum-integral equation is derived using the transformation of Howarth (reference 1) together with a more general viscosity-temperature relation than that used in reference 1. The greater part of the analysis presented follows along the lines of reference 1, but the emphasis herein is placed on simplifying the final results of the analysis so that they can easily be applied to any practical problem.

Although the present analysis is carried out for two-dimensional flows, it can be applied to three-dimensional flows with axial symmetry by using the transformation of Mangler (see appendix A). Under this transformation, a three-dimensional body with a given pressure gradient is transformed to a related two-dimensional body. The results of the present study can be applied to this two-dimensional body.

SYMBOLS

The following symbols are used in this report:

- a speed of sound
- C proportionality factor used in equation (1)
- c_p specific heat at constant pressure
- $f(M_1)$ function defined by equation (28)

$f_1(\lambda)$	function defined by equation (28)
$f_2(\lambda)$	function defined by equation (28)
$f(\eta)$	function defined by equation (20)
h	increment of length
i	summation index
K	arbitrary constant
k	thermal conductivity
M	Mach number
n	transformation variable defined by equation (9)
Pr	Prandtl number, $\mu c_p/k$
p	static pressure
r	radial coordinate
S	Sutherland's constant (216° F)
t	static temperature
u, v	velocity in x - and y -directions, respectively
x, y	cartesian coordinates measured along body and perpendicular to body, respectively
z	function defined by equation (25)
γ	ratio of specific heats
Δ	boundary-layer thickness in x, n coordinate system
Δ^*	function defined by equation (19)
δ	boundary-layer thickness in x, y coordinate system
δ^*	boundary-layer displacement thickness
η	n/Δ

- Θ function defined by equation (18)
- θ boundary-layer momentum thickness
- λ Pohlhausen parameter
- μ absolute viscosity
- ν kinematic viscosity
- ρ mass density
- τ shear stress
- ϕ transformed stream function
- ψ stream function

Subscripts:

- 0 conditions at stagnation point
- 1 conditions at outer edge of boundary layer
- s standard condition
- w condition at solid boundary

ASSUMPTIONS

The following assumptions are made in addition to the usual boundary-layer assumptions in order to make the problem amenable to solution:

- (1) The Prandtl number of the fluid is equal to 1. It has been shown in reference 4 that this assumption has no appreciable effect on flat-plate skin-friction calculations if the fluid is air (for $M < 5$), but the assumption does limit the accuracy of heat-transfer calculations and temperature distributions.
- (2) The heat transfer at the solid boundary is equal to zero. This assumption should be reasonable for many practical applications.

2285 (3) The viscosity and temperature are related linearly by the following expression:

$$\frac{\mu}{\mu_s} = C \frac{t}{t_s} \quad (1)$$

Chapman and Rubesin (reference 5) have shown that solutions of the boundary-layer equations based on equation (1) agree well with reality for flat-plate flows if the constant C is determined by matching equation (1) with Sutherland's relation at the solid boundary so that

$$C = \sqrt{\frac{t_w (t_s + s)}{t_s (t_w + s)}} \quad (2)$$

This assumption should also be reasonable for the case of flows with streamwise pressure gradients because the wall temperature t_w is constant as a consequence of assumptions (1) and (2).

ANALYSIS

Compressible laminar-boundary-layer equations. - The momentum equation describing the flow in the boundary layer is

$$u \frac{\partial u}{\partial x} + v \frac{\partial u}{\partial y} = - \frac{1}{\rho} \frac{\partial p}{\partial x} + \frac{1}{\rho} \frac{\partial}{\partial y} \left(\mu \frac{\partial u}{\partial y} \right) \quad (3)$$

The equation of continuity is

$$\frac{\partial}{\partial x} (\rho u) + \frac{\partial}{\partial y} (\rho v) = 0 \quad (4)$$

The flow of heat is described by the energy equation, which is

$$\rho c_p \left(u \frac{\partial t}{\partial x} + v \frac{\partial t}{\partial y} \right) = u \frac{\partial p}{\partial x} + \frac{\partial}{\partial y} \left(k \frac{\partial t}{\partial y} \right) + \mu \left(\frac{\partial u}{\partial y} \right)^2 \quad (5)$$

A particular solution of the energy equation can be obtained by multiplying equation (3) by ρu and adding the result to equation (5), and by letting the Prandtl number equal 1. This solution is

$$\frac{u^2}{2} + c_p t = \text{constant} \quad (6)$$

and corresponds to the case where the heat transfer at the solid boundary is equal to zero.

The equation of state can be expressed as

$$\frac{p}{p_s} = \frac{\rho}{\rho_s} \frac{t}{t_s} \quad (7)$$

The Bernoulli equation, which applies at the outer edge of the boundary layer, is

$$\frac{dp}{dx} = - \rho_1 u_1 \frac{du_1}{dx} \quad (8)$$

Transformation of Howarth. - In reference 1 Howarth introduces a transformation which, when applied to equation (3), yields an equation similar to the incompressible momentum equation. In the present report the transformation is modified slightly to include the proportionality factor C in equation (1). The transformation variables are

$$\left. \begin{aligned} x &\equiv x \\ n &\equiv \frac{1}{\sqrt{C}} \left(\frac{p}{p_s} \right)^{\frac{1}{2}} \int_0^y \frac{t_s}{t} dy \end{aligned} \right\} \quad (9)$$

where n alters the scale in the direction normal to the surface. The derivatives are expressed as follows:

$$\left. \begin{aligned} \frac{\partial}{\partial x} \Big|_y &= \frac{\partial}{\partial x} \Big|_n + \frac{\partial n}{\partial x} \frac{\partial}{\partial n} \\ \frac{\partial}{\partial y} &= \frac{1}{\sqrt{C}} \left(\frac{p}{p_s} \right)^{\frac{1}{2}} \frac{t_s}{t} \frac{\partial}{\partial n} \end{aligned} \right\} \quad (10)$$

Before transforming equation (3) it is convenient to introduce a stream function $\psi(x, y)$ which satisfies equation (4). This function is defined by

$$\left. \begin{aligned} \rho u &= \rho_s \frac{\partial \psi}{\partial y} \\ \rho v &= - \rho_s \frac{\partial \psi}{\partial x} \end{aligned} \right\} \quad (11)$$

In terms of the transformed coordinate system, a function $\phi(x, n)$ can be defined as

$$\psi(x, y) = \sqrt{C} \left(\frac{p}{p_s} \right)^{\frac{1}{2}} \phi(x, n) \quad (12)$$

From equations (10), (11), and (12),

$$\left. \begin{aligned} u &= \frac{\partial \phi}{\partial n} \\ v &= - \frac{\rho_s}{\rho} \left[\sqrt{\frac{pC}{p_s}} \left(\frac{\partial \phi}{\partial x} + \frac{\partial \phi}{\partial n} \frac{\partial n}{\partial x} \right) + \phi \frac{\partial}{\partial x} \left(\sqrt{\frac{pC}{p_s}} \right) \right] \end{aligned} \right\} \quad (13)$$

and, as shown in reference 1, from equations (1), (7), (8), (10), and (13), the momentum equation becomes

$$\frac{\partial \phi}{\partial n} \frac{\partial^2 \phi}{\partial x \partial n} - \frac{\partial \phi}{\partial x} \frac{\partial^2 \phi}{\partial n^2} - u_1 \frac{du_1}{dx} \left(\frac{t}{t_1} - \frac{r-1}{2a_1^2} \phi \frac{\partial^2 \phi}{\partial n^2} \right) = v_s \frac{\partial^3 \phi}{\partial n^3} \quad (14)$$

The temperature term in this equation can be expressed in the form

$$\frac{t}{t_1} = 1 + \frac{u_1^2 - u^2}{2c_p t_1} = 1 + \frac{r-1}{2} M_1^2 - \frac{r-1}{2a_1^2} \left(\frac{\partial \phi}{\partial n} \right)^2 \quad (15)$$

from which

$$\begin{aligned} \frac{\partial \phi}{\partial n} \frac{\partial^2 \phi}{\partial x \partial n} - \frac{\partial \phi}{\partial x} \frac{\partial^2 \phi}{\partial n^2} - u_1 \frac{du_1}{dx} \left[1 + \frac{r-1}{2} M_1^2 - \frac{r-1}{2a_1^2} \left(\frac{\partial \phi}{\partial n} \right)^2 - \right. \\ \left. \frac{r}{2a_1^2} \phi \frac{\partial^2 \phi}{\partial n^2} \right] = v_s \frac{\partial^3 \phi}{\partial n^3} \end{aligned} \quad (16)$$

With the exception of the term within the bracket, equation (16) is identical in form to the incompressible momentum equation.

Momentum-integral equation. - The momentum-integral equation is obtained by integrating each term of equation (16) from the solid boundary to the outer edge of the boundary layer (see reference 1):

$$u_1^2 \frac{d\Theta}{dx} + u_1 \frac{du_1}{dx} \left[\Theta \left(2 - \frac{M_1^2}{2} \right) + \Delta^* \left(1 + \frac{r-1}{2} M_1^2 \right) \right] = v_s \left(\frac{\partial u}{\partial n} \right)_w \quad (17)$$

where

$$\Theta \equiv \int_0^\Delta \left(1 - \frac{u}{u_1} \right) \frac{u}{u_1} dn \quad (18)$$

$$\Delta^* \equiv \int_0^\Delta \left(1 - \frac{u}{u_1} \right) dn \quad (19)$$

The auxiliary functions Θ and Δ^* are similar to the momentum thickness θ and the displacement thickness δ^* in the physical coordinate system.

Modified Kármán-Pohlhausen solution. - In order to solve equation (17) by the Kármán-Pohlhausen method it is necessary to introduce the variable $\eta \equiv n/\Delta$ and to assume that u/u_1 is a polynomial in η . As in the method of Pohlhausen, this polynomial is taken to be of the fourth degree. The coefficients of the polynomial are determined from the following boundary conditions:

$$n = 0: \quad u = 0$$

$$-u_1 \frac{du_1}{dx} \left(1 + \frac{\gamma-1}{2} M_1^2 \right) = v_s \frac{\partial^3 \phi}{\partial n^3} = v_s \frac{\partial^2 u}{\partial n^2}$$

$$n = \Delta: \quad u = u_1$$

$$\frac{\partial u}{\partial n} = \frac{\partial^2 u}{\partial n^2} = 0$$

Thus the following form is obtained for the velocity profile:

$$\frac{u}{u_1} = f(\eta) = 2\eta - 2\eta^3 + \eta^4 + \lambda \left[\frac{1}{6} \eta (1-\eta)^3 \right] \quad (20)$$

where the parameter λ is defined as

$$\lambda \equiv \frac{\Delta^2}{v_s} \frac{du_1}{dx} \left(1 + \frac{\gamma-1}{2} M_1^2 \right) \quad (21)$$

Transformation to the η -coordinate and subsequent integration in equations (18) and (19) yield

$$\Theta = \frac{\Delta}{315} \left(37 - \frac{\lambda}{3} - \frac{5\lambda^2}{144} \right) \quad (22)$$

$$\Delta^* = \Delta \left(\frac{36 - \lambda}{120} \right) \quad (23)$$

and it is found that

$$\left(\frac{\partial u}{\partial n} \right)_w = \frac{u_1}{\Delta} \left(2 + \frac{\lambda}{6} \right) \quad (24)$$

Equations (22), (23), and (24) could be applied to equation (17) directly and the result would be a differential equation for λ (reference 1). A simpler solution can be obtained by applying the substitution of Holstein-Bohlen:

$$Z = \Theta^2 / v_s \quad (25)$$

or, from equations (22) and (21),

$$Z = \frac{\lambda}{\frac{du_1}{dx} \left(1 + \frac{r-1}{2} M_1^2 \right)} \left[\frac{1}{315} \left(37 - \frac{\lambda}{3} - \frac{5\lambda^2}{144} \right) \right]^2 \quad (26)$$

Equation (17) is multiplied by $\Theta/u_1 v_s$, and equations (25) and (26) are substituted in the resulting expression to yield

$$\frac{u_1}{2} \frac{dZ}{dx} + f_1(\lambda) \left[-f(M_1) + \frac{\Delta^*}{\Theta} \right] = \frac{\Theta}{u_1} \left(\frac{\partial u}{\partial n} \right)_w$$

Then, from equations (22), (23), and (24),

$$\frac{dZ}{dx} = \frac{2}{u_1} \left[f_1(\lambda) f(M_1) + f_2(\lambda) \right] \quad (27)$$

where

$$\left. \begin{aligned} f_1(\lambda) &\equiv \lambda \left[\frac{1}{315} \left(37 - \frac{\lambda}{3} - \frac{5\lambda^2}{144} \right)^2 \right] \\ f_2(\lambda) &\equiv \frac{1}{315} \left(37 - \frac{\lambda}{3} - \frac{5\lambda^2}{144} \right) \left(2 - \frac{2\lambda}{15} + \frac{\lambda^2}{120} \right) \\ f(M_1) &\equiv \frac{M_1^2 - 4}{2 + (\gamma-1) M_1^2} \end{aligned} \right\} \quad (28)$$

and

$$Z = \frac{f_1(\lambda)}{\frac{du_1}{dx} \left(1 + \frac{\gamma-1}{2} M_1^2 \right)} \quad (29)$$

Equations (27) and (29) can now be integrated simultaneously, and λ can be obtained as a function of x by a method of numerical integration given in detail in appendix B. The functions $f_1(\lambda)$ and $f_2(\lambda)$ are graphically presented in figure 1 and are tabulated in table I; $f(M_1)$ is tabulated in table II. Boundary-layer variables are still in the transformed system of coordinates, however, and a transformation to the physical (x, y) coordinates is required.

Inverse transformation to physical coordinates. - The distance normal to the surface can be obtained from equation (9):

$$\begin{aligned} dy &= \sqrt{\frac{p_s C}{p}} \frac{t}{t_s} dn \\ &= \Delta \sqrt{\frac{p_s C}{p}} \frac{t}{t_s} d\eta \end{aligned}$$

or

$$y = \Delta \sqrt{\frac{p_s C}{p}} \frac{t_1}{t_s} \int_0^\eta \frac{t}{t_1} d\eta$$

But, from equation (15),

$$\frac{t}{t_1} = 1 + \frac{r-1}{2} M_1^2 \left[1 - \left(\frac{u}{u_1} \right)^2 \right] \quad (30)$$

and, from equation (20),

$$\frac{t}{t_1} = 1 + \frac{r-1}{2} M_1^2 \left(1 - \sum_{i=2}^8 a_i \eta^i \right) \quad (31)$$

where

$$a_2 = \frac{\lambda^2}{36} + \frac{2}{3} \lambda + 4$$

$$a_3 = - \frac{\lambda^2}{6} - 2\lambda$$

$$a_4 = \frac{5\lambda^2}{12} + \frac{4\lambda}{3} - 8$$

$$a_5 = - \frac{5\lambda^2}{9} + \frac{5\lambda}{3} + 4$$

$$a_6 = \frac{5\lambda^2}{12} - 3\lambda + 4$$

$$a_7 = - \frac{\lambda^2}{6} + \frac{5\lambda}{3} - 4$$

$$a_8 = \frac{\lambda^2}{36} - \frac{\lambda}{3} + 1$$

(The functions a_i are tabulated in table I and presented graphically in fig. 2.)

from which

$$y = \Delta \sqrt{\frac{p_s C}{p}} \frac{t_1}{t_s} \left[\eta \left(1 + \frac{r-1}{2} M_1^2 \right) - \frac{r-1}{2} M_1^2 \sum_{i=2}^8 \frac{a_i \eta^{i+1}}{i+1} \right] \quad (32)$$

where Δ is obtained from equation (21). The boundary-layer thickness is determined by letting η equal 1:

$$\delta = \Delta \sqrt{\frac{p_s C}{p}} \frac{t_1}{t_s} \left[1 + \frac{\gamma-1}{2} M_1^2 (-0.0001\lambda^2 - 0.0094\lambda + 0.4175) \right] \quad (33)$$

The momentum thickness is defined as

2285

$$\begin{aligned} \theta &= \int_0^\delta \frac{\rho u}{\rho_1 u_1} \left(1 - \frac{u}{u_1} \right) dy \\ &= \frac{t_1}{t_s} \sqrt{\frac{p_s C}{p}} \int_0^\Delta \frac{u}{u_1} \left(1 - \frac{u}{u_1} \right) dn \\ &= \frac{t_1}{t_s} \sqrt{\frac{p_s C}{p}} \theta \end{aligned} \quad (34)$$

and the displacement thickness is

$$\begin{aligned} \delta^* &= \int_0^\delta \left(1 - \frac{\rho u}{\rho_1 u_1} \right) dy = \frac{t_1}{t_s} \sqrt{\frac{p_s C}{p}} \left[\int_0^\Delta \left(1 - \frac{u}{u_1} \right) dn + \int_0^\Delta \left(\frac{t}{t_1} - 1 \right) dn \right] \\ &= \frac{t_1}{t_s} \sqrt{\frac{p_s C}{p}} \left[\Delta^* + \Delta \left(\frac{\gamma-1}{2} \right) M_1^2 (-0.0001\lambda^2 - 0.0094\lambda + 0.4175) \right] \end{aligned} \quad (35)$$

The wall shear stress τ_w is defined as

$$\begin{aligned} \tau_w &= \mu \left(\frac{\partial u}{\partial y} \right)_w \\ &= \mu_s \sqrt{\frac{p C}{p_s}} \left(\frac{\partial u}{\partial n} \right)_w \\ &= \frac{u_1 \mu_s}{\Delta} \sqrt{\frac{p C}{p_s}} \left(2 + \frac{\lambda}{6} \right) \end{aligned} \quad (36)$$

The separation point is defined as the point where the shear stress vanishes, or, from equation (36), where $\lambda = -12$. It is emphasized, however, that the Kármán-Pohlhausen solution has been found to be quite inaccurate in the neighborhood of a separation point.

SUMMARY OF METHOD

The results of this study will be summarized in the order they are needed for the solution of a particular problem. It is assumed that all free-stream conditions $(u_1, \frac{du_1}{dx}, M_1, t_1, p_1)$ are known functions of x . The standard conditions (v_s, p_s, t_s) are selected as mean values of the free-stream conditions. Next λ is determined as a function of x by solving equations (27) and (29) numerically:

$$\frac{dZ}{dx} = \frac{2}{u_1} \left[f_1(\lambda) f(M_1) + f_2(\lambda) \right] \quad (27)$$

$$Z = \frac{f_1(\lambda)}{\frac{du_1}{dx} \left(1 + \frac{r-1}{2} M_1^2 \right)} \quad (29)$$

where

$$\left. \begin{aligned} f_1(\lambda) &\equiv \lambda \left[\frac{1}{315} \left(37 - \frac{\lambda}{3} - \frac{5\lambda^2}{144} \right) \right]^2 \\ f_2(\lambda) &\equiv \frac{1}{315} \left(37 - \frac{\lambda}{3} - \frac{5\lambda^2}{144} \right) \left(2 - \frac{2\lambda}{15} + \frac{\lambda^2}{120} \right) \\ f(M_1) &\equiv \frac{M_1^2 - 4}{2 + (r-1) M_1^2} \end{aligned} \right\} \quad (28)$$

A suggested procedure for solving equation (27) is presented in appendix B. All functions of λ and M_1 are tabulated in tables I and II.

Once λ is known as a function of x , the following functions can be found:

$$\Delta = \sqrt{\frac{\lambda v_s}{\frac{du_1}{dx} \left(1 + \frac{r-1}{2} M_1^2 \right)}} \quad (21)$$

$$\Theta = \frac{\Delta}{315} \left(37 - \frac{\lambda}{3} - \frac{5\lambda^2}{144} \right) \quad (22)$$

$$\Delta^* = \Delta \left(\frac{36 - \lambda}{120} \right) \quad (23)$$

and

$$\delta = \Delta \sqrt{\frac{p_s C}{p}} \frac{t_1}{t_s} \left[1 + \frac{r-1}{2} M_1^2 (-0.0001\lambda^2 - 0.0094\lambda + 0.4175) \right] \quad (33)$$

$$\theta = \frac{t_1}{t_s} \sqrt{\frac{p_s C}{p}} \Theta \quad (34)$$

$$\delta^* = \frac{t_1}{t_s} \sqrt{\frac{p_s C}{p}} \left[\Delta^* + \Delta \left(\frac{r-1}{2} \right) M_1^2 (-0.0001\lambda^2 - 0.0094\lambda + 0.4175) \right] \quad (35)$$

$$\tau_w = \frac{u_1 \mu_s}{\Delta} \sqrt{\frac{p C}{p_s}} \left(2 + \frac{\lambda}{6} \right) \quad (36)$$

and, for assumed values of $0 \leq \eta \leq 1$,

$$\frac{u}{u_1} = 2\eta - 2\eta^3 + \eta^4 + \lambda \left[\frac{1}{6} \eta (1-\eta)^3 \right] \quad (20)$$

$$\frac{t}{t_1} = 1 + \frac{r-1}{2} M_1^2 \left[1 - \left(\frac{u}{u_1} \right)^2 \right] \quad (30)$$

The velocity and temperature profiles can then be found in terms of the physical (x, y) coordinate system by the following relation:

$$y = \Delta \sqrt{\frac{p_s C}{p}} \frac{t_1}{t_s} \left[\eta \left(1 + \frac{r-1}{2} M_1^2 \right) - \frac{r-1}{2} M_1^2 \sum_{i=2}^8 \frac{a_i \eta^{i+1}}{i+1} \right] \quad (32)$$

where

$$a_2 = \frac{\lambda^2}{36} + \frac{2}{3} \lambda + 4$$

$$a_3 = -\frac{\lambda^2}{6} - 2\lambda$$

$$a_4 = \frac{5\lambda^2}{12} + \frac{4\lambda}{3} - 8$$

$$a_5 = -\frac{5\lambda^2}{9} + \frac{5\lambda}{3} + 4$$

$$a_6 = \frac{5\lambda^2}{12} - 3\lambda + 4$$

$$a_7 = -\frac{\lambda^2}{6} + \frac{5\lambda}{3} - 4$$

$$a_8 = \frac{\lambda^2}{36} - \frac{\lambda}{3} + 1$$

SPECIAL CASES

Solution near a stagnation point. - In the immediate neighborhood of a stagnation point, u_1 is equal to zero and the incompressible solution must apply. This solution is (reference 3):

$$\left. \begin{aligned} \lambda_0 &= 7.052 \\ z_0 &= \frac{0.077}{du_1/dx} \\ \left(\frac{dz}{dx} \right)_0 &= -0.0652 \frac{d^2u_1/dx^2}{du_1/dx} \end{aligned} \right\} \quad (37)$$

Flat-plate solution. - In the case of the flat plate, $\lambda = 0$ and the conditions at the outer edge of the boundary layer are constant and equal to the standard condition(s). Equation (27) therefore becomes

$$\frac{dz}{dx} = \frac{2}{u_1} \left[f_1(0) f(M_1) + f_2(0) \right]$$

$$= \frac{0.470}{u_1}$$

and

$$z = \frac{0.470 x}{u_1} \quad (38)$$

From equations (25) and (34), the momentum thickness is

$$\theta = 0.685 \sqrt{\frac{v_1 x C}{u_1}} \quad (39)$$

The boundary-layer thickness is found from equations (22), (34), and (33) to be

$$\delta = 5.836 \sqrt{\frac{v_1 x C}{u_1}} \left[1 + 0.417 M_1^2 \left(\frac{r-1}{2} \right) \right] \quad (40)$$

The displacement thickness, from equations (23) and (35), is

$$\delta^* = 1.75 \sqrt{\frac{v_1 x C}{u_1}} \left[1 + 1.392 \left(\frac{r-1}{2} \right) M_1^2 \right] \quad (41)$$

and, from equation (36), the wall shearing stress is found to be

$$\tau_w = \frac{u_1 \mu_1}{2.918} \sqrt{\frac{u_1 C}{v_1 x}} \quad (42)$$

Velocity and temperature profiles can be found as functions of η by letting λ vanish in equations (20) and (30), respectively. The relation of η and y can then be obtained from equation (32). The error introduced in the flat-plate solution by assuming that the velocity profile is a fourth-degree polynomial can be deduced by comparing these results with the results of reference 5:

$$\theta = 0.664 \sqrt{\frac{v_1 x C}{u_1}} \quad (43)$$

$$\delta^* = 1.73 \sqrt{\frac{v_1 x C}{u_1}} \left[1 + 1.372 \left(\frac{\gamma-1}{2} \right) M_1^2 \right] \quad (44)$$

$$\tau_w = \frac{\mu_1 u_1}{3.02} \sqrt{\frac{u_1 C}{v_1 x}} \quad (45)$$

Equations (43) and (45) apply for any Prandtl number, whereas equation (44) applies for $Pr = 1$ only.

It can therefore be seen that the results of the present analysis are quite accurate for the case of zero pressure gradient. No definite conclusions for the nonzero pressure gradient case can be made, however.

Lewis Flight Propulsion Laboratory
 National Advisory Committee for Aeronautics
 Cleveland, Ohio, August 8, 1951

APPENDIX A

TRANSFORMATION OF MANGLER

The laminar-boundary-layer equations for three-dimensional flows with axial symmetry are

$$\bar{u} \frac{\partial \bar{u}}{\partial \bar{x}} + \bar{v} \frac{\partial \bar{u}}{\partial \bar{y}} = - \frac{1}{\rho} \frac{dp}{dx} + \frac{1}{\rho} \frac{\partial}{\partial \bar{y}} \left(\bar{\mu} \frac{\partial \bar{u}}{\partial \bar{y}} \right) \quad (A1)$$

$$\frac{\partial}{\partial \bar{x}} (\bar{\rho} r_0 \bar{u}) + \frac{\partial}{\partial \bar{y}} (\bar{\rho} r_0 \bar{v}) = 0 \quad (A2)$$

$$\bar{\rho} c_p \left[\bar{u} \frac{\partial \bar{t}}{\partial \bar{x}} + \bar{v} \frac{\partial \bar{t}}{\partial \bar{y}} \right] = \bar{u} \frac{\partial \bar{p}}{\partial \bar{x}} + \frac{\partial}{\partial \bar{y}} \left(\bar{k} \frac{\partial \bar{t}}{\partial \bar{y}} \right) + \bar{\mu} \left(\frac{\partial \bar{u}}{\partial \bar{y}} \right)^2 \quad (A3)$$

where the bar is used to differentiate the three-dimensional from the two-dimensional quantities, and $r_0(x)$ defines the radial coordinate of the body in a meridional plane. The continuity equation is satisfied by the following stream function:

$$r_0 \bar{\rho} \bar{u} = \frac{\partial \bar{\psi}}{\partial \bar{y}} \quad (A4)$$

$$r_0 \bar{\rho} \bar{v} = - \frac{\partial \bar{\psi}}{\partial \bar{x}}$$

The following transformation variables were introduced by Mangler (unavailable report):

$$\left. \begin{aligned} x &= K^2 \int_0^{\bar{x}} r_0^2(\bar{x}) d\bar{x} \\ y &= K r_0(\bar{x}) \bar{y} \end{aligned} \right\} \quad (A5)$$

where K is an arbitrary constant. Thus

$$\frac{\partial}{\partial \bar{x}} = K^2 r_0^2 \frac{\partial}{\partial x} + \frac{y r_0'}{r_0} \frac{\partial}{\partial y}$$

$$\frac{\partial}{\partial \bar{y}} = K r_0 \frac{\partial}{\partial y}$$

where the prime indicates differentiation with respect to \bar{x} .

It is further assumed that

$$\bar{p}(\bar{x}, \bar{y}) = p(x, y)$$

$$\bar{t}(\bar{x}, \bar{y}) = t(x, y)$$

$$\bar{\mu}(\bar{x}, \bar{y}) = \mu(x, y)$$

$$\bar{\rho}(\bar{x}, \bar{y}) = \rho(x, y)$$

$$\bar{\psi}(\bar{x}, \bar{y}) = \frac{1}{K} \psi(x, y)$$

Equations (A1), (A2), and (A3) can then be transformed to the following form:

$$u \frac{\partial u}{\partial x} + v \frac{\partial u}{\partial y} = - \frac{1}{\rho} \frac{dp}{dx} + \frac{1}{\rho} \frac{\partial}{\partial y} \left(\mu \frac{\partial u}{\partial y} \right) \quad (A6)$$

$$\frac{\partial}{\partial x} (\rho u) + \frac{\partial}{\partial y} (\rho v) = 0 \quad (A7)$$

$$\rho c_p \left(u \frac{\partial t}{\partial x} + v \frac{\partial t}{\partial y} \right) = u \frac{\partial p}{\partial x} + \frac{\partial}{\partial y} \left(K \frac{\partial t}{\partial y} \right) + \mu \left(\frac{\partial u}{\partial y} \right)^2 \quad (A8)$$

where

$$u(x, y) = \bar{u}(\bar{x}, \bar{y}) \quad (A9)$$

$$v(x, y) = \frac{1}{K r_0} \left[\bar{v}(\bar{x}, \bar{y}) - \frac{y r_0'}{K r_0^2} \bar{u}(\bar{x}, \bar{y}) \right]$$

Equations (A6), (A7), and (A8) are now identical to equations (3), (4), and (5). The solution of these equations, as presented in the text of

this report, therefore applies to the three-dimensional problem, but the final results must be retransformed to the three-dimensional quantities. The boundary-layer thickness δ is not defined in a solution of the differential boundary-layer equations, but its definition is required for the solution of the integral equation. The transformation of δ can best be accomplished by examining the velocity profiles:

2285

$$\frac{u}{u_1} = \frac{u}{u_1} \left(\frac{y}{\delta} \right)$$

$$\frac{\bar{u}}{\bar{u}_1} = \frac{\bar{u}}{\bar{u}_1} \left(\frac{\bar{y}}{\delta} \right)$$

From equation (A9), however,

$$\frac{u}{u_1} = \frac{\bar{u}}{\bar{u}_1}$$

It therefore follows that

$$\frac{y}{\delta} = \frac{\bar{y}}{\delta}$$

whence, from equation (A5),

$$\delta = Kr_0(\bar{x}) \bar{\delta} \quad (A10)$$

The momentum thickness is transformed as follows:

$$\bar{\theta}(\bar{x}) = \int_0^{\bar{\delta}} \frac{\bar{u}}{\bar{u}_1} \left(1 - \frac{\bar{\rho} \bar{u}}{\bar{\rho}_1 \bar{u}_1} \right) d\bar{y}$$

$$= \frac{1}{Kr_0} \int_0^{\delta} \frac{u}{u_1} \left(1 - \frac{\rho u}{\rho_1 u_1} \right) dy$$

$$= \frac{1}{Kr_0} \theta(x) \quad (A11)$$

and similarly,

$$\left. \begin{aligned} \bar{\delta}^*(\bar{x}) &= \frac{1}{K r_0} \delta^*(x) \\ \bar{\tau}_w(\bar{x}) &= K r_0 \tau_w(x) \end{aligned} \right\} \quad (A12)$$

where the quantities without the bar (representing two-dimensional quantities) are given by equations (33) to (36).

Therefore, if it is desired to determine any of the boundary-layer characteristics at a distance \bar{x} from the nose of an axially symmetric body, the corresponding two-dimensional distance x is first found from equation (A5). The two-dimensional quantities (δ , δ^* , θ , τ_w , and so forth) are then found using equations (33) to (36), and are transformed to the three-dimensional quantities at \bar{x} through the use of equations (A10) to (A12). The transformation applies for flows with or without streamwise pressure gradients.

APPENDIX B

SOLUTION OF DIFFERENTIAL EQUATION BY RUNGE-KUTTA METHOD

The Runge-Kutta method of finite differences (reference 6) has been found to be very satisfactory for solving equation (27). It is believed that a detailed discussion of the method, as applied to the present problem, will be of help to the reader.

It is suggested that a table of the following form be used:

	(1)	(2)	(3)	(4)	(5)	(6)	(7)	(8)	(9)	(10)	(11)
	x	u_1	$\frac{du_1}{dx}$	M_1	$f(M_1)$	$1 + \frac{\gamma-1}{2} M_1^2$	Z	$f_1(\lambda)$	λ	$f_2(\lambda)$	k
1	0						Z_0				k_1
2	$h/2$						$Z_0 + \frac{1}{2} k_1$				k_2
3	$h/2$						$Z_0 + \frac{1}{2} k_2$				k_3
4	h						$Z_0 + k_3$				k_4
5	h						Z_1				k_1
6	$h + \frac{h}{2}$						$Z_1 + \frac{1}{2} k_1$				k_2
7	$h + \frac{h}{2}$						$Z_1 + \frac{1}{2} k_2$				k_3
8	$2h$						$Z_1 + k_3$				k_4

The distance along the body (x) is subdivided into a number of increments h , and the free-stream variables u_1 , du_1/dx , and M_1 at each point are tabulated in columns (2), (3), and (4). Column (5) follows from equation (28), and column (6) is easily tabulated. Columns (1) to (6) can be tabulated for all x , whereas for columns (7) to (11), each row must be calculated separately.

The value of $Z_0 = \Theta_0^2/v_s$ (column (7), row 1) is given by equation (37) for stagnation-point flow, or is equal to zero if $\Theta_0 = 0$. The value of $f_1(\lambda)$ (column 8) is obtained from equation (29), or in column notation,

$$f_1(\lambda) = (7)(3)(6)$$

Columns (9) and (10) are obtained from figure (1). Column (11) lists the Runge-Kutta parameter k , which in column notation is

$$k = \frac{2}{(2)} \left((8)(5) + (10) \right) h$$

Rows 1 to 4 can now be completed in this manner. At the completion of row 4 the total increment in Z can be computed using the following equation:

$$\Delta Z = \frac{1}{6} (k_1 + 2k_2 + 2k_3 + k_4)$$

The entire process is then repeated for rows 5 to 8. The value of Z_1 (column (7), row 5) is equal to $Z_0 + \Delta Z$. The procedure is carried out for all increments of x , and as a result λ is obtained as a function of x .

REFERENCES

1. Howarth, L.: Concerning the Effect of Compressibility on Laminar Boundary Layers and Their Separation. Proc. Roy. Soc. (London), ser. A, vol. 194, no. A1036, July 28, 1948, pp. 16-42.
2. Lees, Lester: The Stability of the Laminar Boundary Layer in a Compressible Fluid. NACA Rep. 876, 1947. (Formerly NACA TN 1360.)
3. Schlichting, H.: Lecture Series "Boundary Layer Theory." Part I - Laminar Flows. NACA TM 1217, 1949, pp. 93-100.
4. Rubesin, M. W., and Johnson, H. A.: A Critical Review of Skin-Friction and Heat-Transfer Solutions of the Laminar Boundary Layer of a Flat Plate. Trans. A.S.M.E., vol. 71, no. 4, May 1949, pp. 383-388.
5. Chapman, Dean R., and Rubesin, Morris W.: Temperature and Velocity Profiles in the Compressible Laminar Boundary Layer with Arbitrary Distribution of Surface Temperature. Jour. Aero. Sci., vol. 16, no. 9, Sept. 1949, pp. 547-565.
6. Scarborough, James B.: Numerical Mathematical Analysis. Johns Hopkins Press (Baltimore), 1930, pp. 273-274.

TABLE I - FUNCTIONS OF λ

λ	$f_1(\lambda)$	$f_2(\lambda)$	a_2	a_3	a_4	a_5	a_6	a_7	a_8	$-0.0001\lambda^2$ -0.0094 λ +0.4175	Δ^*/Δ	θ/Δ	$2 + \lambda/6$
12	0.0948	0.1422	16.000	-48.000	68.000	-56.000	28.000	-8.000	1.000	0.2888	0.2000	0.0889	4.000
11	.0941	.1426	14.695	-42.167	57.084	-44.889	21.417	-5.833	.694	.3008	.2083	.0925	3.833
10	.0920	.1438	13.444	-36.667	47.000	-34.889	15.667	-4.000	.445	.3125	.2167	.0958	3.667
9	.0882	.1461	12.250	-31.500	37.750	-26.000	10.750	-2.500	.250	.3240	.2250	.0990	3.500
8	.0831	.1495	11.111	-26.667	29.334	-18.221	6.667	-1.333	.111	.3353	.2333	.1019	3.333
7	.0767	.1544	10.028	-22.167	21.750	-11.556	3.417	-.500	.028	.3463	.2417	.1047	3.167
6	.0689	.1608	9.000	-18.000	15.000	-6.000	1.000	0	0	.3572	.2500	.1071	3.000
5	.0599	.1687	8.028	-14.167	9.084	-1.555	-.583	.167	.028	.3678	.2583	.1094	2.833
4	.0497	.1784	7.111	-10.667	4.000	1.778	-.1.333	0	.111	.3782	.2667	.1115	2.667
3	.0385	.1898	6.250	-7.500	-.250	4.000	-.1.250	-.500	.250	.3883	.2750	.1133	2.500
2	.0264	.2030	5.445	-4.667	-3.667	5.111	-.333	-.1.333	.445	.3983	.2833	.1149	2.333
1	.0135	.2181	4.694	-2.167	-6.250	5.111	1.417	-.2.500	.694	.4080	.2917	.1163	2.167
0	0	.2350	4.000	0	-8.000	4.000	4.000	4.000	1.000	.4175	.3000	.1175	2.000
-1	-.0140	.2536	3.361	1.833	-8.917	1.778	7.417	-.5.833	1.361	.4268	.3083	.1184	1.833
-2	-.0284	.2742	2.778	3.333	-9.000	-.1.555	11.667	-.8.000	1.778	.4358	.3167	.1191	1.667
-3	-.0429	.2963	2.250	4.500	-8.250	-.6.000	16.750	-.10.500	2.250	.4447	.3250	.1197	1.500
-4	-.0575	.3200	1.778	5.333	-6.667	-.11.556	22.667	-.13.333	2.778	.4533	.3333	.1199	1.133
-5	-.0720	.3450	1.361	5.833	-4.250	-.18.221	29.417	-.16.500	3.361	.4617	.3417	.1200	1.167
-6	-.0862	.3717	1.000	6.000	-1.000	-.26.000	37.000	-.20.000	4.000	.4699	.3500	.1198	1.000
-7	-.0999	.3992	.695	5.833	3.084	-34.889	45.417	-.23.833	4.694	.4778	.3583	.1195	.833
-8	-.1130	.4279	.444	5.333	8.000	-44.889	54.667	-.28.000	5.445	.4855	.3667	.1189	.667
-9	-.1255	.4576	.250	4.500	13.750	-.56.000	64.750	-.32.500	6.250	.4930	.3750	.1181	.500
-10	-.1369	.4874	.111	3.333	20.333	-.68.222	75.667	-.37.333	7.111	.5003	.3833	.1170	.333
-11	-.1474	.5181	.028	1.833	27.750	-.81.556	87.417	-.42.500	8.028	.5074	.3917	.1158	.167
-12	-.1567	.5486	0	36.000	0	100.000	-.48.000	9.000	0	.5142	.4000	.1143	0



TABLE II - FUNCTIONS OF M_1 $[\gamma = 1.40]$

M_1	$\frac{\gamma-1}{2} M_1^2$	$1 + \frac{\gamma-1}{2} M_1^2$	$f(M_1)$	M_1	$\frac{\gamma-1}{2} M_1^2$	$1 + \frac{\gamma-1}{2} M_1^2$	$f(M_1)$
0	0	1.000	-2.000	2.2	0.968	1.968	0.213
.2	.008	1.008	-1.974	2.4	1.152	2.152	.409
.4	.032	1.032	-1.861	2.6	1.352	2.352	.589
.6	.072	1.072	-1.698	2.8	1.568	2.568	.748
.8	.128	1.128	-1.489	3.0	1.800	2.800	.893
1.0	.200	1.200	-1.250	3.2	2.048	3.048	1.024
1.2	.288	1.288	-.994	3.4	2.312	3.312	1.141
1.4	.392	1.392	-.733	3.6	2.592	3.592	1.247
1.6	.512	1.512	-.476	3.8	2.880	3.880	1.343
1.8	.648	1.648	-.231	4.0	3.200	4.200	1.500
2.0	.800	1.800	0				



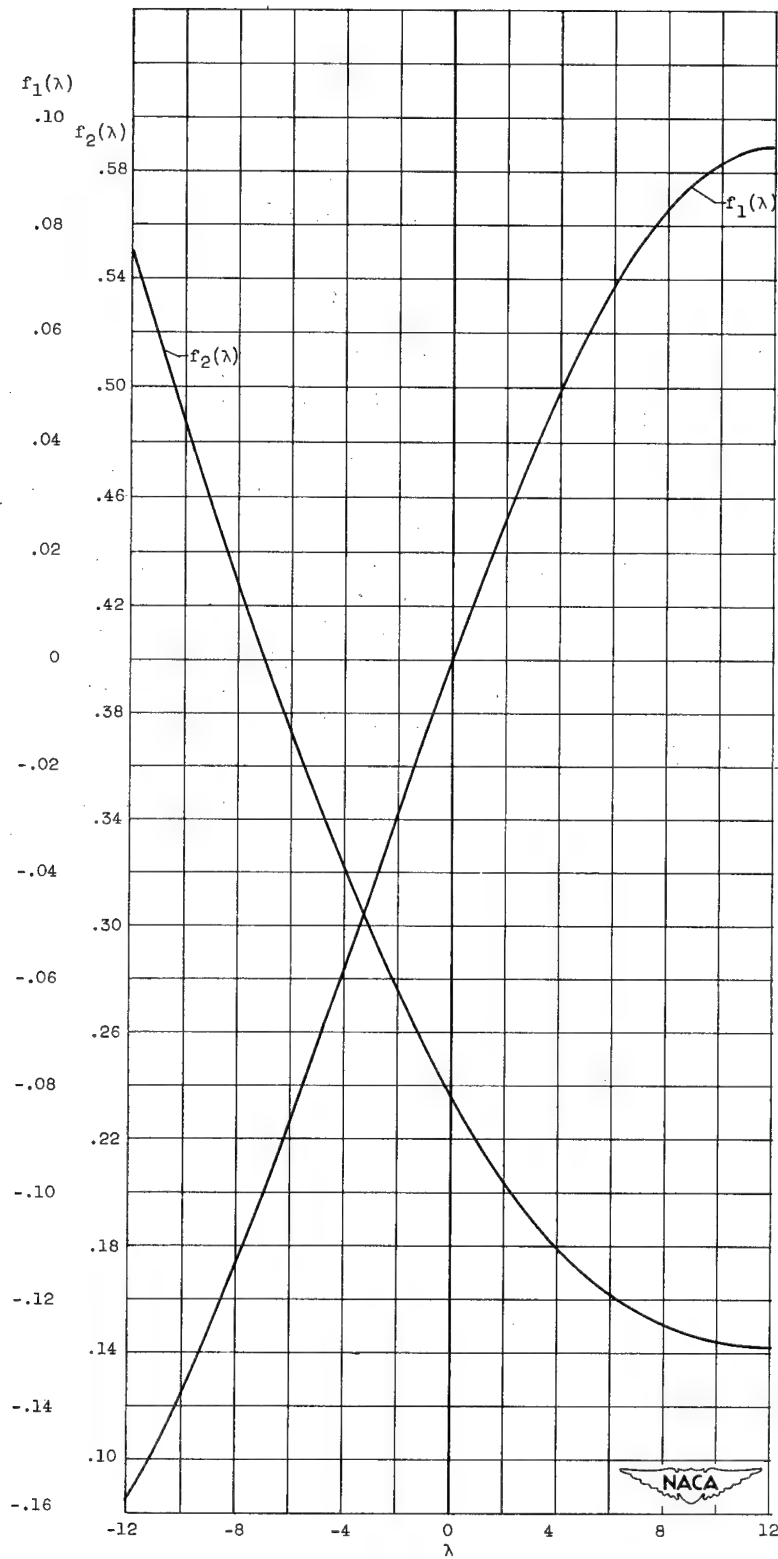


Figure 1. - Auxiliary functions used in equation (27).

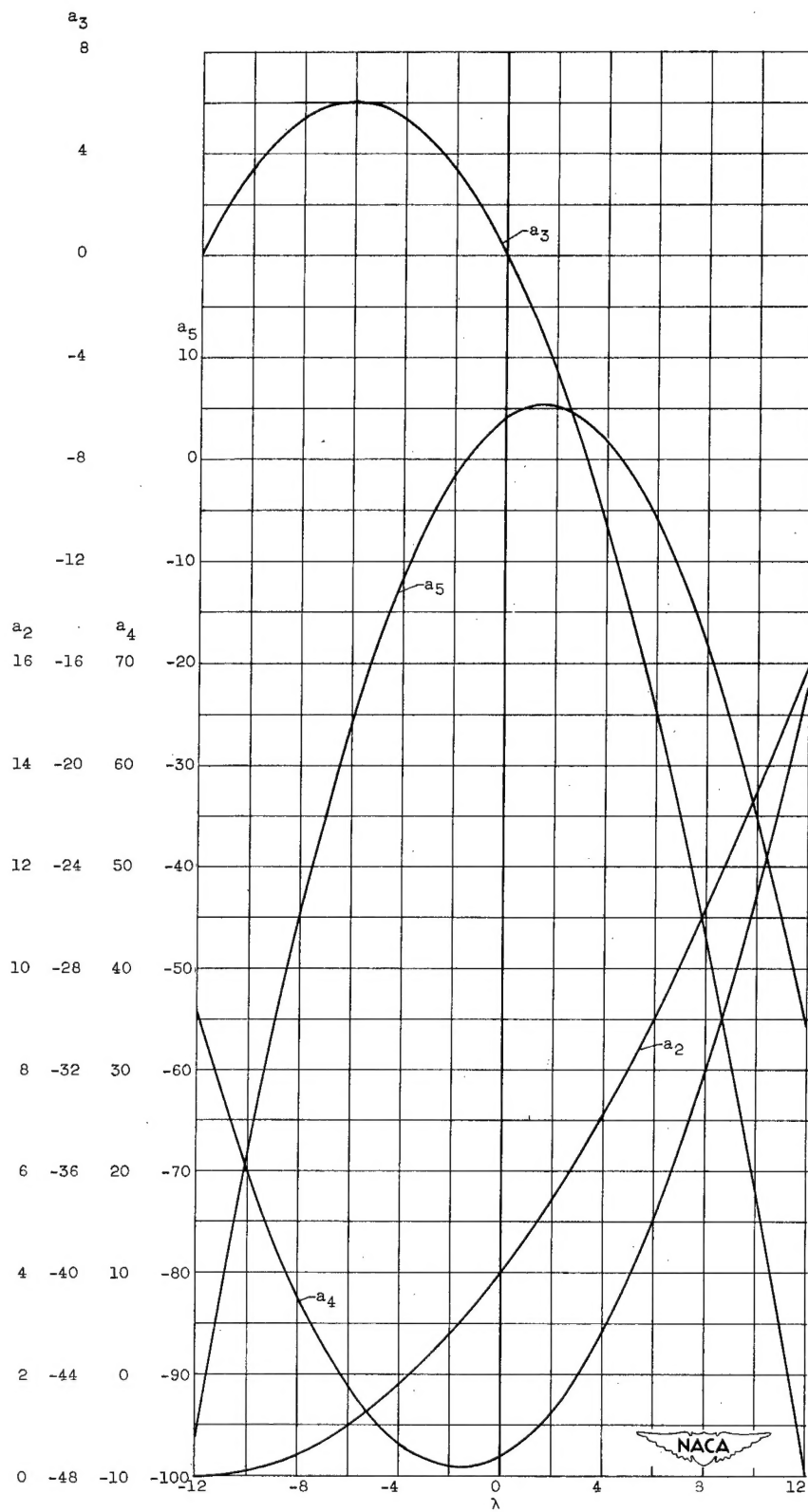


Figure 2. - Auxiliary functions used in equations (31) and (32).

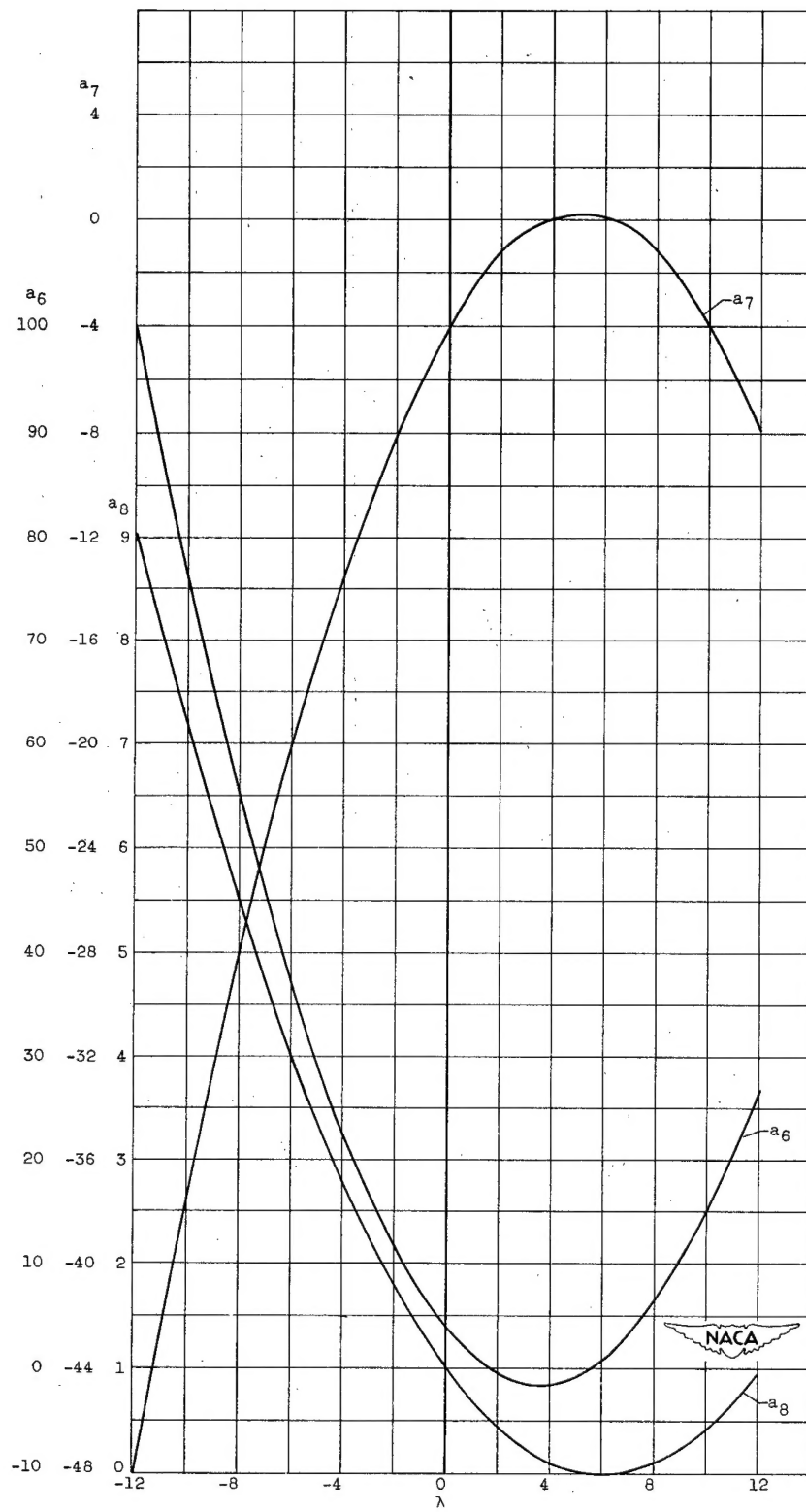


Figure 2. - Concluded. Auxiliary functions used in equations (31) and (32).

<p>NACA TN 2531 National Advisory Committee for Aeronautics. SIMPLIFIED METHOD FOR CALCULATION OF COMPRESSIBLE LAMINAR BOUNDARY LAYER WITH ARBITRARY FREE-STREAM PRESSURE GRADIENT. George M. Low. October 1951. 28p. diagrs., 2 tabs. (NACA TN 2531)</p> <p>The Kármán-Polhausen method, as applied to compressible laminar boundary layers, is simplified by an analysis similar to the incompressible Holstein-Bohlen method. The analysis is carried out under the assumptions of a Prandtl number of 1, zero heat transfer, and a linear viscosity-temperature relation. Results are presented so that velocity and temperature profiles, momentum and displacement thicknesses, and wall shear stress can be calculated for flows over two-dimensional bodies with arbitrary free-stream velocity distributions. The results are also applicable to flows over three-dimensional(over)</p> <p>Copies obtainable from NACA, Washington</p>	<p>NACA TN 2531 National Advisory Committee for Aeronautics. SIMPLIFIED METHOD FOR CALCULATION OF COMPRESSIBLE LAMINAR BOUNDARY LAYER WITH ARBITRARY FREE-STREAM PRESSURE GRADIENT. George M. Low. October 1951. 28p. diagrs., 2 tabs. (NACA TN 2531)</p> <p>The Kármán-Polhausen method, as applied to compressible laminar boundary layers, is simplified by an analysis similar to the incompressible Holstein-Bohlen method. The analysis is carried out under the assumptions of a Prandtl number of 1, zero heat transfer, and a linear viscosity-temperature relation. Results are presented so that velocity and temperature profiles, momentum and displacement thicknesses, and wall shear stress can be calculated for flows over two-dimensional bodies with arbitrary free-stream velocity distributions. The results are also applicable to flows over three-dimensional(over)</p> <p>Copies obtainable from NACA, Washington</p>
<p>NACA TN 2531 National Advisory Committee for Aeronautics. SIMPLIFIED METHOD FOR CALCULATION OF COMPRESSIBLE LAMINAR BOUNDARY LAYER WITH ARBITRARY FREE-STREAM PRESSURE GRADIENT. George M. Low. October 1951. 28p. diagrs., 2 tabs. (NACA TN 2531)</p> <p>The Kármán-Polhausen method, as applied to compressible laminar boundary layers, is simplified by an analysis similar to the incompressible Holstein-Bohlen method. The analysis is carried out under the assumptions of a Prandtl number of 1, zero heat transfer, and a linear viscosity-temperature relation. Results are presented so that velocity and temperature profiles, momentum and displacement thicknesses, and wall shear stress can be calculated for flows over two-dimensional bodies with arbitrary free-stream velocity distributions. The results are also applicable to flows over three-dimensional(over)</p> <p>Copies obtainable from NACA, Washington</p>	<p>NACA TN 2531 National Advisory Committee for Aeronautics. SIMPLIFIED METHOD FOR CALCULATION OF COMPRESSIBLE LAMINAR BOUNDARY LAYER WITH ARBITRARY FREE-STREAM PRESSURE GRADIENT. George M. Low. October 1951. 28p. diagrs., 2 tabs. (NACA TN 2531)</p> <p>The Kármán-Polhausen method, as applied to compressible laminar boundary layers, is simplified by an analysis similar to the incompressible Holstein-Bohlen method. The analysis is carried out under the assumptions of a Prandtl number of 1, zero heat transfer, and a linear viscosity-temperature relation. Results are presented so that velocity and temperature profiles, momentum and displacement thicknesses, and wall shear stress can be calculated for flows over two-dimensional bodies with arbitrary free-stream velocity distributions. The results are also applicable to flows over three-dimensional(over)</p> <p>Copies obtainable from NACA, Washington</p>

NACA TN 2531

bodies with axial symmetry through the use of
Mangler's transformation.

NACA TN 2531

bodies with axial symmetry through the use of
Mangler's transformation.



Copies obtainable from NACA, Washington

Copies obtainable from NACA, Washington

NACA TN 2531

bodies with axial symmetry through the use of
Mangler's transformation.

NACA TN 2531

bodies with axial symmetry through the use of
Mangler's transformation.



Copies obtainable from NACA, Washington

Copies obtainable from NACA, Washington

